

Tunable white-light emission in single-phased $\text{K}_2\text{Y}_{1-x}\text{Eu}_x\text{Zr}(\text{PO}_4)_3$ phosphor

Liang Shi and Hyo Jin Seo*

Department of Physics, Pukyong National University, Busan 608-737, Korea

*hjseo@pknu.ac.kr

Abstract: The single-phased $\text{K}_2\text{Y}_{1-x}\text{Eu}_x\text{Zr}(\text{PO}_4)_3$ ($x = 0\sim 1$) phosphors were prepared by solid-state reaction. The greenish-blue Zr^{4+} -emission due to the $\text{Zr}^{4+}\text{-O}^{2-}$ charge transfer transition is observed in the $\text{K}_2\text{YZr}(\text{PO}_4)_3$ ($x = 0$) phosphor under UV excitation. Together with the Zr^{4+} -emission, the red emission of Eu^{3+} is progressively developed by replacement of Y^{3+} to Eu^{3+} over the full Eu-content ($x = 0\sim 1$) in $\text{K}_2\text{Y}_{1-x}\text{Eu}_x\text{Zr}(\text{PO}_4)_3$. The emission color varies from greenish-blue to whitish with increasing Eu^{3+} -content and the white-light emission is realized in single-phased phosphor of $\text{K}_2\text{EuZr}(\text{PO}_4)_3$ ($x = 1$) by combining the Zr^{4+} -emission and the Eu^{3+} -emission.

©2011 Optical Society of America

OCIS codes: (160.4670) Optical materials; (160.4760) Optical properties; (160.5690) Rare-earth-doped materials; (300.6280) Spectroscopy, fluorescence and luminescence.

References and links

1. H. Guo, X. F. Wang, J. D. Chen, and F. Li, "Ultraviolet light induced white light emission in Ag and Eu^{3+} co-doped oxyfluoride glasses," *Opt. Express* **18**(18), 18900–18905 (2010).
2. P. Babu, K. H. Jang, Ch. S. Rao, L. Shi, C. K. Jayasankar, V. Lavín, and H. J. Seo, "White light generation in Dy^{3+} -doped oxyfluoride glass and transparent glass-ceramics containing CaF_2 nanocrystals," *Opt. Express* **19**(3), 1836–1841 (2011).
3. W.-J. Yang and T.-M. Chen, "White-light generation and energy transfer in $\text{SrZn}_2(\text{PO}_4)_2\text{:Eu,Mn}$ phosphor for ultraviolet light-emitting diodes," *Appl. Phys. Lett.* **88**, 1019031 (2006).
4. X. Liu, C. Lin, and J. Lin, "White light emission from Eu^{3+} in CaIn_2O_4 host lattices," *Appl. Phys. Lett.* **90**(8), 081904 (2007).
5. N. Guo, H. You, Y. Song, M. Yang, K. Liu, Y. Zheng, Y. Huang, and H. Zhang, "White-light emission from a single-emitting-component $\text{Ca}_9\text{Gd}(\text{PO}_4)_7\text{:Eu}^{2+},\text{Mn}^{2+}$ phosphor with tunable luminescent properties for near-UV light-emitting diodes," *J. Mater. Chem.* **20**(41), 9061–9067 (2010).
6. E. Danielson, M. Devenney, D. M. Giaquinta, J. H. Golden, R. C. Haushalter, E. W. McFarland, D. M. Pojary, C. M. Reaves, W. H. Weinberg, and X. D. Wu, "A rare-earth phosphor containing one-dimensional chains identified through combinatorial methods," *Science* **279**(5352), 837–839 (1998).
7. G. Blasse, G. Bernardi, D. J. W. IJdo, and J. R. Plaisier, "Yellow zirconate luminescence in $\text{Ca}_3\text{ZrSi}_2\text{O}_9$," *J. Alloy. Comp.* **217**(1), 29–30 (1995).
8. Y. Takahashi, K. Kitamura, N. Iyi, and S. Inoue, "Visible orange photoluminescence in a barium titanosilicate $\text{BaTiSi}_2\text{O}_7$," *Appl. Phys. Lett.* **88**(15), 151903 (2006).
9. M. Kaneyoshi, "Luminescence of some zirconium-containing compounds under vacuum ultraviolet excitation," *J. Lumin.* **121**(1), 102–108 (2006).
10. L. Zhang, G. Y. Hong, and X. L. Sun, "The luminescence of the phosphor Sr_2ZrO_4 with one-dimensional chains structure," *Chin. Chem. Lett.* **10**, 799–802 (1999).
11. G. Blasse, J. de Blank, and D. J. W. IJdo, "The luminescence of the garnet $\text{Ca}_4\text{ZrGe}_3\text{O}_{12}$," *Mater. Res. Bull.* **30**(7), 845–850 (1995).
12. L. Li, S. Zhou, and S. Zhang, "Investigation on charge transfer bands of Ce^{4+} in Sr_2CeO_4 blue phosphor," *Chem. Phys. Lett.* **453**(4-6), 283–289 (2008).
13. S. A. Basun, T. Danger, A. A. Kaplyanskii, D. S. McClure, K. Petermann, and W. C. Wong, "Optical and photoelectrical studies of charge-transfer processes in $\text{YAlO}_3\text{:Ti}$ crystals," *Phys. Rev. B Condens. Matter* **54**(9), 6141–6149 (1996).
14. W. C. Wong, T. Danger, G. Huber, and K. Petermann, "Spectroscopy and excited-state absorption of $\text{Ti}^{4+}\text{:Li}_4\text{Ge}_5\text{O}_{12}$ and $\text{Ti}^{4+}\text{:Y}_2\text{SiO}_5$," *J. Lumin.* **72–74**, 208–210 (1997).
15. I. V. Ogorodnyk, I. V. Zatovsky, and N. S. Slobodyanik, "Rietveld refinement of langbeinite-type $\text{K}_2\text{YHf}(\text{PO}_4)_3$," *Acta Crystallogr. Sect. E Struct. Rep. Online* **65**(8), i63–i64 (2009).
16. I. G. Trubach, A. I. Beskrovnyi, A. I. Orlova, V. A. Orlova, and V. S. Kurazhkovskaya, "Synthesis and investigation of the new phosphates $\text{K}_2\text{LnZr}(\text{PO}_4)_3$ ($\text{Ln}=\text{Ce}-\text{Yb}$, Y) with langbeinite structure," *Crystallogr. Rep.* **49**(4), 614–618 (2004).
17. Q. Sun and J. Shi, "Calculation and prediction the charge transfer energy of $\text{O}^{2-}-\text{Zr}^{4+}$ in inorganic crystals," *J. Phys. Chem. C* **114**(7), 3230–3234 (2010).

18. D. L. Dexter, "A theory of sensitized luminescence in solids," J. Chem. Phys. **21**(5), 836–851 (1953).
19. S. P. Feofilov, Y. Zhou, H. J. Seo, J. Y. Jeong, D. A. Keszler, and R. S. Meltzer, "Host sensitization of Gd³⁺ ions in yttrium and scandium borates and phosphates: application to quantum cutting," Phys. Rev. B **74**(8), 085101 (2006).

1. Introduction

The phosphors with white-light emission have attracted much attention for their application in white-light near-UV LEDs. Recently white-light generation has been achieved in glasses [1,2] and phosphors [3–6]. The formation of phosphors with single phase is one of the important factors because of their excellent color rendering indexes and the electro-optical design being simple to control the different colors in comparison to mixed (red, green, and blue) phosphors [3–5]. White-light emission can be generated in phosphors codoped with two types of activators via energy transfer processes, for examples, in SrZn₂(PO₄)₂:Eu²⁺,Mn²⁺ [3] and Ca₉Gd(PO₄)₇:Eu²⁺,Mn²⁺ [5]. The luminescence with blue-white color was also realized in fully concentrated Ce-based Sr₂CeO₄ phosphor [6]. Fully concentrated phosphors can offer benefits in terms of easy preparation without formation of substitutional defects.

The broad UV-visible emissions have been reported in compounds with tetravalent (M⁴⁺) cations such as Zr⁴⁺, Ce⁴⁺, and Ti⁴⁺ in which the M⁴⁺-O²⁻ charge transfer (M-O CT) transition is responsible for the emissions [6–11]. The M-O CT transition takes place uniquely from the M⁴⁺ ions with octahedral coordination of oxygen ions. The Ce⁴⁺ ions in Sr₂CeO₄ form chains of edge-sharing CeO₆ octahedra in which the cerium centers with two terminal oxygen atoms are isolated from one another by Sr²⁺ cations [6]. This structural anisotropy of Sr₂CeO₄ gives rise to the Ce⁴⁺-emission with maximum at 485 nm due to the Ce-O CT transition [6,12]. The M-O CT blue-emissions are generated in YAlO₃ [13] and Li₄Ge₅O₁₂ [14] doped with the Ti⁴⁺ ions replacing the Al and Ge ions at octahedral sites, respectively. The Zr⁴⁺-emissions at low temperature were reported in Ca₃ZrSi₂O₉ [7] and Sr₂ZrO₄ [10] with the emission maxima at UV (320 nm) and yellow (540 nm) regions, respectively. However, the visible Zr⁴⁺-emission at room temperature has been rarely reported probably because of thermal quenching in the host lattices. In this study, we report the Zr⁴⁺-emission in the visible region and the tunable white-light emission in single-phased K₂Y_{1-x}Eu_xZr(PO₄)₃ phosphors under UV excitation at room temperature.

2. Experimental

The K₂Y_{1-x}Eu_xZr(PO₄)₃ (x = 0~1) phosphors with langbeinite structure were prepared by solid-state reaction method. Stoichiometric amounts of high purity (Aldrich, >99.9%) K₂CO₃, ZrO₂, NH₄H₂PO₄, Y₂O₃ and Eu₂O₃ were thoroughly mixed and heated at 1200 °C for 20 h in air. Crystalline phases of samples were measured by X-ray diffraction (Philips, X'Pert-MPD System). The luminescence excitation and emission spectra were recorded on a Photon Technology International (PTI) fluorimeter at room temperature. The excitation and emission spectra were compared to those of reference sample of sodium salicylate to estimate the quantum yield of the samples.

3. Results and discussion

Figure 1 shows the typical X-ray diffraction (XRD) patterns of the K₂YZr(PO₄)₃ (x = 0) and K₂EuZr(PO₄)₃ (x = 1) phosphors. The patterns are in good agreement with standard card (JCPDs No. 49-0633). From the Rietveld refinement it is found that the lattice parameter *a* and cell volume *V* increase monotonically with Eu³⁺-contents from 10.288 to 10.309 Å and from 1,088.91 to 1,095.59 Å³, respectively. This indicates that the phosphors form a solid solution of K₂Y_{1-x}Eu_xZr(PO₄)₃ over the full range of Eu³⁺-content.

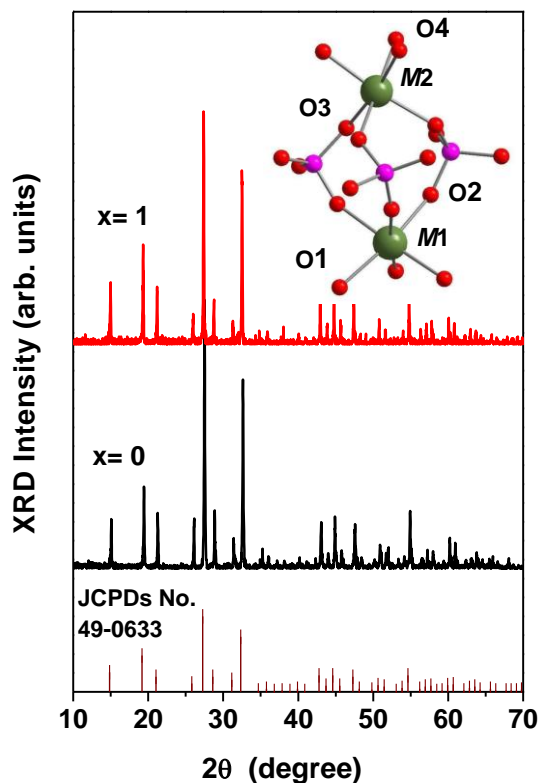


Fig. 1. XRD patterns of the $K_2Y_{1-x}Eu_xZr(PO_4)_3$ ($x = 0$ and 1) phosphors and the structural fragment $\{M_2(PO_4)_3\}$ of $K_2YZr(PO_4)_3$.

The broad emission band in the greenish-blue region with a maximum at 475 nm under the excitation at 320 nm is observed for $K_2YZr(PO_4)_3$ (Fig. 2(a)). The excitation band obtained by monitoring the 475 nm emission has a maximum at around 320 nm (Fig. 2(a)). Considering the langbeinite structure of $K_2YZr(PO_4)_3$, the framework $\{M_2(PO_4)_3\}$ builds up from two MO_6 ($M = Y$ and Zr) octahedra and three PO_4 tetrahedra, which are connected via vertices as shown in the top of Fig. 1. Potassium cations are in the structural cages. All MO_6 octahedra are separated from each other. The Y^{3+} and Zr^{4+} cations are statistically distributed in MO_6 octahedra. The difference in bond length of M1-O1 (2.28 Å), M1-O2 (2.26 Å), M2-O3 (2.20 Å), and M2-O4 (2.03 Å) induces a directional sloping of MO_6 octahedra which leads to shift the M ions from the center of octahedron [15,16]. As a result, the acentric symmetry of the ZrO_6 octahedron changes the distribution of charge density derived from the oxygen ligands [17]. This causes a polarization in the ZrO_6 octahedron and allows the emission due to the Zr-O CT transition under UV excitation. The larger polarization effect pushes the energy state of the Zr-O CT transition down to longer wavelengths (visible). This is the reason why the visible emission is observed in the samples under study. Furthermore, the YO_6 octahedra isolate a ZrO_6 octahedron from the others resulting in localization of the Zr-O CT state reducing luminescence quenching by energy migration.

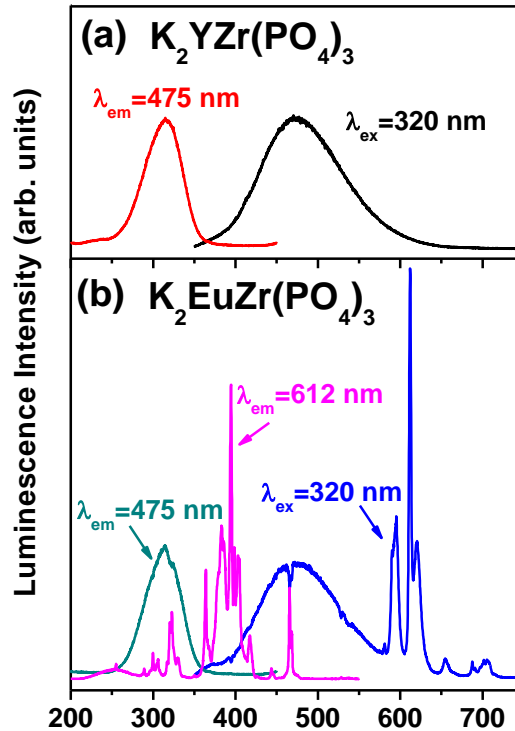


Fig. 2. Excitation and emission spectra of the $\text{K}_2\text{YZr}(\text{PO}_4)_3$ (a) and $\text{K}_2\text{EuZr}(\text{PO}_4)_3$ (b) phosphors at room temperature. The excitation and monitoring wavelengths are indicated.

Together with the broad Zr^{4+} -emission band the strong Eu^{3+} -emission lines are observed in the spectrum of $\text{K}_2\text{EuZr}(\text{PO}_4)_3$ ($x = 1$) (Fig. 2(b)). The excitation spectrum of the Zr^{4+} -emission (475 nm) in $\text{K}_2\text{EuZr}(\text{PO}_4)_3$ ($x = 1$) shows nearly the same spectral feature as that in $\text{K}_2\text{YZr}(\text{PO}_4)_3$ ($x = 0$). But the excitation spectrum of the Eu^{3+} -emission (615 nm) is different from that of the Zr^{4+} -emission in which the excitation lines are attributed to the intra-4f transitions of Eu^{3+} .

The emission spectra ($\lambda_{\text{ex}} = 320$ nm) for different Eu-content are shown in Fig. 3(a). No luminescence quenching is observed as Eu^{3+} -content increases. The dips at around 466 nm are observed in the emission spectra (Figs. 3(a) and 2(b)) of Eu-doped $\text{K}_2\text{YZr}(\text{PO}_4)_3$. The dips become slightly larger with increasing Eu-content. The absorption of the Zr-O CT luminescence by the Eu^{3+} ions is responsible for the dips through the energy transfer process. With increasing Eu^{3+} -content, the Zr^{4+} -emission (475 nm) decreases in intensity and that of the Eu^{3+} -emission increases (Fig. 3(b)). As shown in Fig. 2(b), the emission band of the Zr-O CT state overlaps the excitation lines of Eu^{3+} . This spectral overlap gives rise to energy transfer from the Zr-O CT state to the Eu^{3+} ions resulting in changes in intensity ratio of $\text{Eu}^{3+}/\text{Zr-O CT}$ for different Eu-content.

The excitation and emission spectra of each sample were compared to that of a reference sample of sodium salicylate whose absolute quantum efficiency is assumed to be about 58% and constant over the excitation wavelength range from 140 to 340 nm [18,19]. The sodium salicylate shows broad band-emission with maximum at 420 nm and half width of 65 nm. The

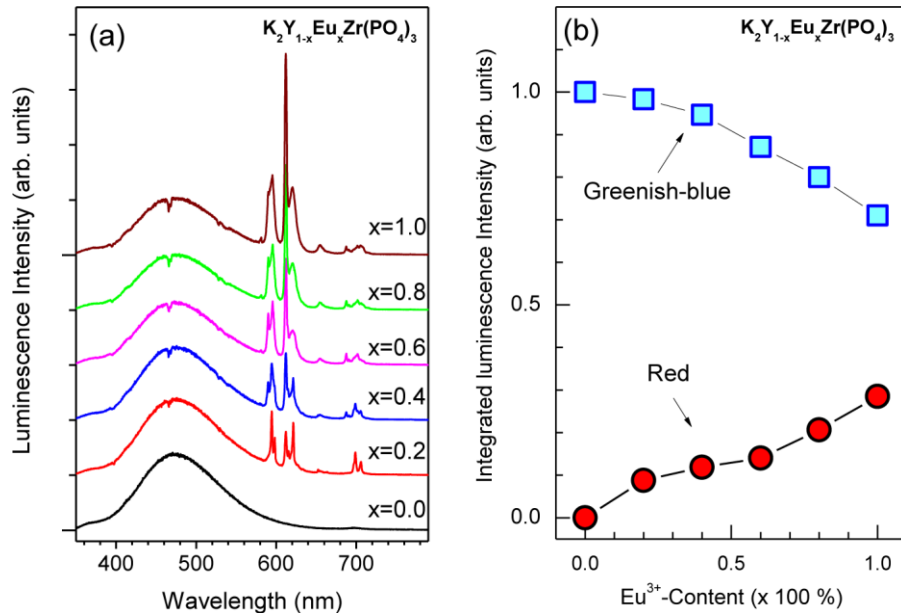


Fig. 3. (a) Emission spectra of the $K_2Y_{1-x}Eu_xZr(PO_4)_3$ ($x = 0 \sim 1$) phosphors for various amounts of Eu^{3+} under 320 nm excitation at room temperature. (b) The integrated intensity of the Zr^{4+} -emission (square) and Eu^{3+} -emission (circle).

luminescence intensity of $K_2YZr(PO_4)_3$ obtained by monitoring the Eu^{3+} - and Zr-O CT emissions ($\lambda_{em} > 350$ nm) under the 320 nm excitation was detected to be about 26% of sodium salicylate. Under the same conditions ($\lambda_{ex} = 320$ nm and $\lambda_{em} > 350$ nm) as $K_2YZr(PO_4)_3$, the emission intensity of sodium salicylate was compared with that of $K_2YZr(PO_4)_3$. As a consequence, the quantum yields of $K_2YZr(PO_4)_3$ is estimated to be about 15%. For the Eu-doped samples the quantum yield is slightly different from sample to sample due to the different absorption for each composition but no significant change in efficiency was estimated. We confirmed that the luminescence intensity of $K_2Y_{1-x}Eu_xZr(PO_4)_3$ at 18 K is about 1.5 times stronger than that at room temperature. The thermal quenching of the luminescence in the $K_2Y_{1-x}Eu_xZr(PO_4)_3$ lattice at various temperature will be reported elsewhere.

Figure 4 shows the Commission Internationale de l'Éclairage (CIE) 1931 chromaticity diagram for single-phased $K_2Y_{1-x}Eu_xZr(PO_4)_3$ phosphors excited at 320 nm, in which the points 1-6 are assigned to Eu^{3+} -contents of $x = 0, 0.2, 0.4, 0.6, 0.8,$ and 1.0 , respectively. By increasing Eu^{3+} -content, the emission changes in color from greenish-blue (point 1) to white (point 6) without doping other luminescence centers in the host lattice. The photographs of the $K_2YZr(PO_4)_3$ (point 1) and $K_2EuZr(PO_4)_3$ (point 6) phosphors under 320 nm excitation are shown at the top right in Fig. 4. Remarkably, the $K_2Y_{1-x}Eu_xZr(PO_4)_3$ ($x = 0.8$ and 1) phosphors show white luminescence to the naked eyes and the CIE color coordinates are $(x = 0.28, y = 0.28)$ and $(x = 0.31, y = 0.28)$, respectively.

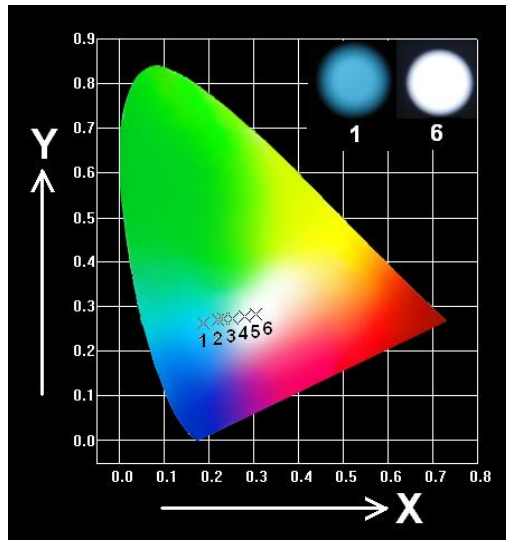


Fig. 4. The CIE chromaticity diagram for $K_2Y_{1-x}Eu_xZr(PO_4)_3$ ($x = 0-1$) phosphors excited at 320 nm. The upper inset is the luminescent photography of $K_2YZr(PO_4)_3$ (point 1) and $K_2EuZr(PO_4)_3$ (point 6) phosphors. The photographs of the $K_2YZr(PO_4)_3$ (point 1) and $K_2EuZr(PO_4)_3$ (point 6) phosphors under 320 nm excitation are shown at the top right.

4. Conclusion

The $K_2YZr(PO_4)_3$ phosphor generates the greenish-blue emission with maximum at 475 nm due to the Zr-O CT transition under the UV excitation at 320 nm. The mechanism of the Zr-O CT transition that is proposed here suggests the shift of charge densities of Zr^{4+} and oxygen ligands from center of octahedron in $K_2YZr(PO_4)_3$. The emission color of the $K_2Y_{1-x}Eu_xZr(PO_4)_3$ phosphors is tuned by changing Eu^{3+} -content and the white-light emission at $x = 1$ is realized by combining the Zr^{4+} -emission (greenish-blue) with the Eu^{3+} emission (red). We believe that this system is useful to understand the tetravalent CT transition.

The bright white-light realized in this phosphor indicates that it can be applied in the lighting and displaying under UV excitation. A shift of excitation-band maximum toward longer wavelength can be achieved by partial substitution of host cations in the lattice by foreign cations with either larger or smaller ionic radii for practical application in white-light near UV-LEDs. Further study in this regard is now in progress. The excitation and emission bands of the Zr-O CT transition depend strongly on the crystal structure of host lattice. Thus it deserves to investigate new Zr^{4+} -compounds with similar lattice structure to $K_2YZr(PO_4)_3$.

Acknowledgments

This work was supported by Mid-career Researcher Program through National Research Foundation of Korea (NRF) grant funded by the Ministry of Education, Science and Technology (MEST) (Project No. 2009-0078682). Thanks are due to Professor Yanlin Huang (Soochow University) for very useful discussions and for reading the manuscript.